Status of the Mainz muon $g-2$ programme

Simon Kuberski for the Mainz lattice group

Lattice Gauge Theory Contributions to New Physics Searches
Instituto de Fisica Teorica (IFT) UAM/CSIC Madrid
June 12, 2023

HIM HELMHOLTZ
Helmholtz-Institut Mainz

- Magnetic moment of a particle with charge e, mass m and spin $\vec{s}$:

$$\vec{\mu} = g \cdot \frac{e}{2m} \cdot \vec{s}$$

- Quantum corrections lead to deviations from the classical value $g = 2$ (Dirac) for elementary particles with $s_z = \hbar/2$, the anomalous magnetic moment

$$a = \frac{g-2}{2} = \frac{\alpha}{2\pi} + \mathrm{O}(\alpha^2) \quad \text{(Schwinger)}$$

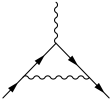

- Anomalous magnetic moments may be determined very precisely, for the electron one finds [2209.13084, Fan et al.]:

$$a_e = 0.001\,159\,652\,180\,59(13)\,.$$

"The most precise prediction of the SM agrees with the most precise determination of a property of an elementary particle to about 1 part in 10^{12}."

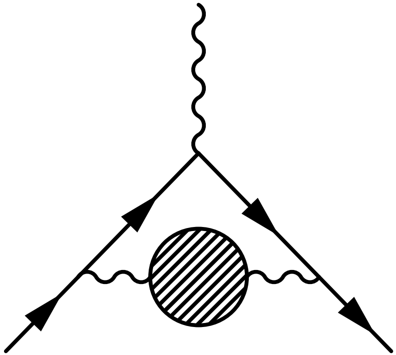

hadronic vacuum polarization

- SM prediction from QED, electroweak and hadronic contributions:

$$a_l^{\mathrm{SM}} = a_l^{\mathrm{QED}} + a_l^{\mathrm{EW}} + a_l^{\mathrm{had}}$$

where $a_l^{\mathrm{had}} = a_\mu^{\mathrm{hvp}} + a_\mu^{\mathrm{hlbl}}$.

- Contributions from new physics at some scale Λ_{NP} enter a_l for $l \in \{e, \mu, \tau\}$ via

$$a_l - a_l^{\mathrm{SM}} \propto \frac{m_l^2}{\Lambda_{\mathrm{NP}}^2}$$

where a_τ is inaccessible for experiment and $m_\mu / m_e \approx 207$.

Contribution	Value $\times 10^{11}$
Experiment (E821 + E989)	$116\,592\,061(41)$
HVP LO (e^+e^-)	$6931(40)$
HVP NLO (e^+e^-)	$-98.3(7)$
HVP NNLO (e^+e^-)	$12.4(1)$
HVP LO (lattice, $udsc$)	$7116(184)$
HLbL (phenomenology)	$92(19)$
HLbL NLO (phenomenology)	$2(1)$
HLbL (lattice, uds)	$79(35)$
HLbL (phenomenology + lattice)	$90(17)$
QED	$116\,584\,718.931(104)$
Electroweak	$153.6(1.0)$
HVP (e^+e^-, LO + NLO + NNLO)	$6845(40)$
HLbL (phenomenology + lattice + NLO)	$92(18)$
Total SM Value	$116\,591\,810(43)$
Difference: $\Delta a_\mu := a_\mu^{\text{exp}} - a_\mu^{\text{SM}}$	$251(59)$

- Theory initiative: Status for a_μ [2203.15810, Colangelo et al.].
- $4.2\,\sigma$ discrepancy between experiment and SM prediction.

Contribution	Value $\times 10^{11}$
Experiment (E821 + E989)	116 592 061(41)
HVP LO (e^+e^-)	6931$\boxed{(40)}$
HVP NLO (e^+e^-)	−98.3(7)
HVP NNLO (e^+e^-)	12.4(1)
HVP LO (lattice, *udsc*)	7116(184)
HLbL (phenomenology)	92(19)
HLbL NLO (phenomenology)	2(1)
HLbL (lattice, *uds*)	79(35)
HLbL (phenomenology + lattice)	90(17)
QED	116 584 718.931(104)
Electroweak	153.6(1.0)
HVP (e^+e^-, LO + NLO + NNLO)	6845(40)
HLbL (phenomenology + lattice + NLO)	92(18)
Total SM Value	116 591 810$\boxed{(43)}$
Difference: $\Delta a_\mu := a_\mu^{\text{exp}} - a_\mu^{\text{SM}}$	251(59)

- Theory initiative: Status for a_μ [2203.15810, Colangelo et al.].
- $4.2\,\sigma$ discrepancy between experiment and SM prediction.
- Uncertainty from $a_\mu^{\text{hvp,LO}}$ dominates a_μ.

Contribution	Value $\times 10^{11}$
Experiment (E821 + E989)	$116\,592\,061(41)$
$\boxed{\text{HVP LO } (e^+e^-)}$	$\boxed{6931(40)}$
HVP NLO (e^+e^-)	$-98.3(7)$
HVP NNLO (e^+e^-)	$12.4(1)$
$\boxed{\text{HVP LO (lattice, } udsc)}$	$\boxed{7116(184)}$
HLbL (phenomenology)	$92(19)$
HLbL NLO (phenomenology)	$2(1)$
HLbL (lattice, uds)	$79(35)$
HLbL (phenomenology + lattice)	$90(17)$
QED	$116\,584\,718.931(104)$
Electroweak	$153.6(1.0)$
HVP (e^+e^-, LO + NLO + NNLO)	$6845(40)$
HLbL (phenomenology + lattice + NLO)	$92(18)$
Total SM Value	$116\,591\,810(43)$
Difference: $\Delta a_\mu := a_\mu^{\text{exp}} - a_\mu^{\text{SM}}$	$251(59)$

- Theory initiative: Status for a_μ [2203.15810, Colangelo et al.].
- $4.2\,\sigma$ discrepancy between experiment and SM prediction.
- Uncertainty from $a_\mu^{\text{hvp,LO}}$ dominates a_μ.
- Lattice result $a_\mu^{\text{hvp,LO}} = 7075(55) \cdot 10^{-11}$ [2002.12347, BMWc] not included in white paper average [2006.04822, Aoyama et al.].

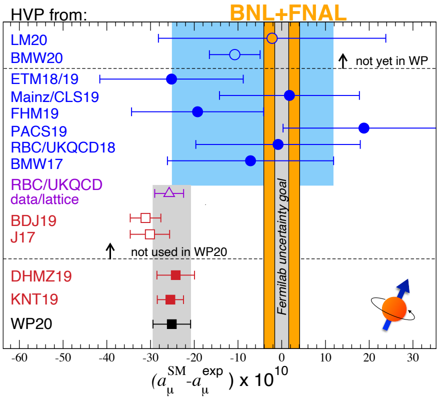

← Status for a_μ^{hvp} [2203.15810, Colangelo et al.]

- Prediction in [2002.12347, BMWc] deviates **significantly** from data-driven results.
- Recent data for $e^+e^- \to \pi^+\pi^-$ [2302.08834, CMD-3] favor shift of data-driven results towards experimental result.
- Additional precise lattice results needed!

- Short term: Focus on benchmark quantities to compare among collaborations. Time windows in the Time Momentum Representation [1801.07224, Blum et al.].
- Long term: Improve overall precision of a_μ^{hvp}.

Hadronic light-by-light scattering

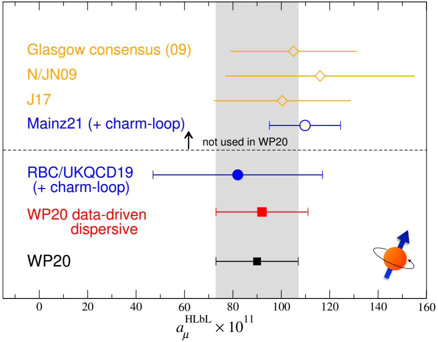

← Status for a_μ^{hlbl} [2203.15810, Colangelo et al.]

- White paper recommended value:

$$a_\mu^{\mathrm{hlbl}} = (92 \pm 18) \cdot 10^{-11}$$

- Recent lattice calculation (Mainz21):

$$a_\mu^{\mathrm{hlbl}} = (109.6 \pm 14.7) \cdot 10^{-11}$$

[2104.02632, 2204.08844, Chao et al.].

- Not shown here: $a_\mu^{\mathrm{hlbl}} = (124.7 \pm 14.9) \cdot 10^{-11}$ [2304.04423, RBC/UKQCD].
- Probably not the reason for tensions between SM and experiment.

a_μ^{hvp} ON THE LATTICE

a_μ^{hvp} ON THE LATTICE

- Relevant quantity on the lattice: The polarization tensor

$$\Pi_{\mu\nu}(Q) = \int \mathrm{d}^4x\, \mathrm{e}^{iQ\cdot x} \langle j_\mu^{\mathrm{em}}(x)\, j_\nu^{\mathrm{em}}(0)\rangle = (Q_\mu Q_\nu - \delta_{\mu\nu} Q^2)\Pi(Q^2)$$

with the electromagnetic current $j_\mu^{\mathrm{em}} = \frac{2}{3}\bar{u}\gamma_\mu u - \frac{1}{3}\bar{d}\gamma_\mu d - \frac{1}{3}\bar{s}\gamma_\mu s + \frac{2}{3}\bar{c}\gamma_\mu c + \ldots$

- Compute a_μ^{hvp} from [Laurup et al.] [hep-lat/0212018, Blum]

$$a_\mu^{\mathrm{hvp}} = \left(\frac{\alpha}{\pi}\right)^2 \int_0^\infty \mathrm{d}Q^2 f(Q^2)\hat{\Pi}(Q^2)\,, \qquad \text{with} \quad \hat{\Pi}(Q^2) = 4\pi^2\left[\Pi(Q^2) - \Pi(0)\right]$$

and a known QED kernel function $f(Q^2)$.

- $\hat{\Pi}$ admits an integral representation in terms of the spatially summed (zero momentum) vector correlator $G(t)$ [1107.4388, Bernecker and Meyer],

$$\Pi(Q^2) - \Pi(0) = \frac{1}{Q^2}\int_0^\infty \mathrm{d}t\, G(t)\left[Q^2t^2 - 4\sin^2\left(\frac{1}{2}Qt\right)\right].$$

Time-momentum representation [1107.4388, Bernecker and Meyer]:

$$(a_\mu^{\mathrm{hvp}}) \;:=\; \left(\frac{\alpha}{\pi}\right)^2 \int_0^\infty dt\, G(t)\widetilde{K}(t)$$

where $\widetilde{K}(t)$ is the QED kernel function

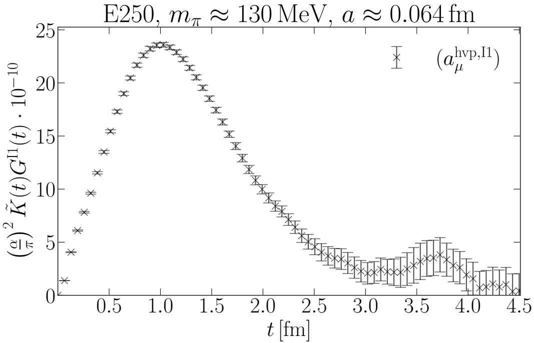

- Current-current correlator:

  $G(t) = -\frac{a^3}{3} \sum_{k=1}^{3} \sum_{\vec{x}} \langle j_k^{\mathrm{em}}(t,\vec{x})\, j_k^{\mathrm{em}}(0)\rangle$

Time-momentum representation [1107.4388, Bernecker and Meyer]:

$$(a_\mu^{\mathrm{hvp}})^i := \left(\frac{\alpha}{\pi}\right)^2 \int_0^\infty dt\, G(t)\widetilde{K}(t) W^i(t;t_0;t_1)$$

where $\widetilde{K}(t)$ is the QED kernel function

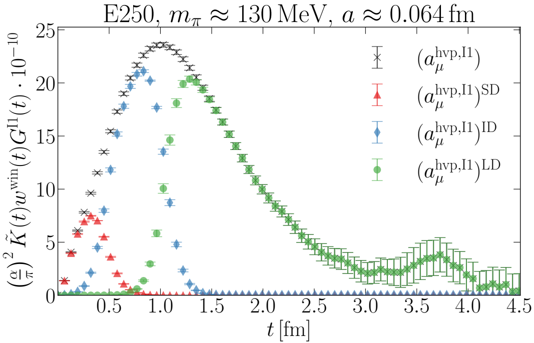

- Current-current correlator:

$$G(t) = -\frac{a^3}{3}\sum_{k=1}^{3}\sum_{\vec{x}} \langle j_k^{\mathrm{em}}(t,\vec{x})\, j_k^{\mathrm{em}}(0)\rangle$$

- Time windows [1801.07224, Blum et al.]:

$$W^{\mathrm{SD}}(t;t_0;t_1) = [1-\Theta(t,t_0,\Delta)]$$
$$W^{\mathrm{ID}}(t;t_0;t_1) = [\Theta(t,t_0,\Delta) - \Theta(t,t_1,\Delta)]$$
$$W^{\mathrm{LD}}(t;t_0;t_1) = \Theta(t,t_0,\Delta)$$

where

$$\Theta(t,t',\Delta) := \tfrac{1}{2}\left(1+\tanh[(t-t')/\Delta]\right)$$
$$t_0 = 0.4\,\mathrm{fm},\ t_1 = 1.0\,\mathrm{fm},\ \Delta = 0.15\,\mathrm{fm}.$$

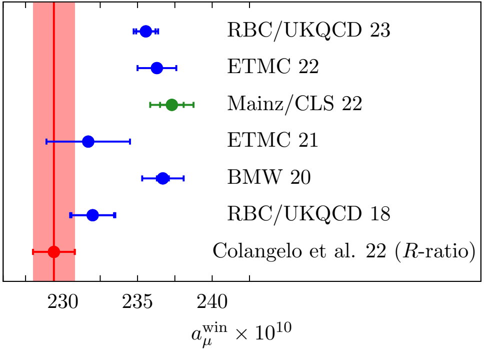

- 3.9σ tension with data-driven estimate in [2205.12963, Colangelo et al.].
- Genuine difference between lattice and data-driven results?
- Recent data-driven analysis of $a_\mu^{\rm win}$ based on τ data agrees with lattice results [2305.20005, Masjuan et al.].

The Mainz/CLS setup

a_μ^{hvp} from $2+1$ flavors of $\mathrm{O}(a)$ improved Wilson-clover fermions

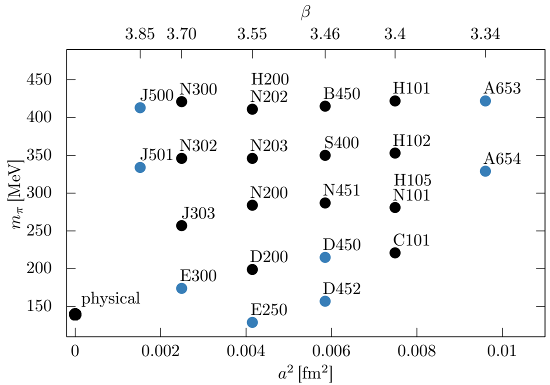

- $\mathrm{O}(a)$ improved Wilson-clover fermions.
- Six values of $a \in [0.039, 0.099]$ fm, a factor of 6.4 in a^2.
- Open boundary conditions in temporal direction.
- $a\mathrm{Tr}[M_\mathrm{q}] = 2am_\mathrm{l} + am_\mathrm{s} = \mathrm{const.}$
- New ensemble / improved statistics since 2019.

Scale: Either use $\sqrt{t_0^\mathrm{phys}} = 0.1443(15)$ fm [2112.06696, Straßberger et al.] or express dimensionfull quantities in terms of af_π [1103.4818, Xu et al.][1904.03120, Gérardin et al.]

$\rightarrow$ new result [2211.03744, Bali et al.]: $\sqrt{t_0^\mathrm{phys}} = 0.1449^{(7)}_{(9)}$ fm may be used in the future.

- Work in isospin decomposition of the electromagnetic current

$$j_\mu^{\mathrm{em}} = \tfrac{2}{3}\bar{u}\gamma_\mu u - \tfrac{1}{3}\bar{d}\gamma_\mu d - \tfrac{1}{3}\bar{s}\gamma_\mu s + \tfrac{2}{3}\bar{c}\gamma_\mu c + \ldots \quad = j_\mu^{I=1} + j_\mu^{I=0} + \tfrac{2}{3}\bar{c}\gamma_\mu c + \ldots, ,$$

Isovector: $j_\mu^{I=1} = \frac{1}{2}(\bar{u}\gamma_\mu u - \bar{d}\gamma_\mu d)$, Isoscalar: $j_\mu^{I=0} = \frac{1}{6}(\bar{u}\gamma_\mu u + \bar{d}\gamma_\mu d - 2\bar{s}\gamma_\mu s)$

- Two discretizations of the vector current: local and conserved

$$J_\mu^{(\mathrm{L}),a}(x) = \overline{\psi}(x)\gamma_\mu \frac{\lambda^a}{2}\psi(x)\,,$$

$$J_\mu^{(\mathrm{C}),a}(x) = \frac{1}{2}\left(\overline{\psi}(x+a\hat{\mu})(1+\gamma_\mu)U_\mu^\dagger(x)\frac{\lambda^a}{2}\psi(x) - \overline{\psi}(x)(1-\gamma_\mu)U_\mu(x)\frac{\lambda^a}{2}\psi(x+a\hat{\mu})\right)\,,$$

- Improved vector currents are given by

$$J_\mu^{(\alpha),a,\mathrm{I}}(x) = J_\mu^{(\alpha),a}(x) + a c_\mathrm{V}^{(\alpha)}(g_0)\,\tilde{\partial}_\nu \Sigma_{\mu\nu}^a(x)\,, \qquad \text{with} \quad \alpha \in \mathrm{L},\mathrm{C}$$

- Renormalization and mass-dependent improvement of local currents via

$$J_\mu^{(\mathrm{L}),3,\mathrm{R}}(x) = Z_\mathrm{V}\left[1 + 3\bar{b}_\mathrm{V} a m_\mathrm{q}^\mathrm{av} + b_\mathrm{V} a m_{\mathrm{q},l}\right] J_\mu^{(\mathrm{L}),3,\mathrm{I}}(x)\,,$$

$$J_\mu^{(\mathrm{L}),8,\mathrm{R}}(x) = Z_\mathrm{V}\left[1 + 3\bar{b}_\mathrm{V} a m_\mathrm{q}^\mathrm{av} + \frac{b_\mathrm{V}}{3} a(m_{\mathrm{q},l} + 2m_{\mathrm{q},s})\right] J_\mu^{(\mathrm{L}),8,\mathrm{I}}(x)$$
$$+ Z_\mathrm{V}\left(\frac{1}{3} b_\mathrm{V} + f_\mathrm{V}\right)\frac{2}{\sqrt{3}} a(m_{\mathrm{q},l} - m_{\mathrm{q},s})\, J_\mu^{(\mathrm{L}),0,\mathrm{I}}(x)\,,$$

- Two independent non-perturbative determinations of $Z_\mathrm{V}, c_\mathrm{V}^L, c_\mathrm{V}^C, b_\mathrm{V}, \bar{b}_\mathrm{V}$:

Set 1: Large-volume, CLS ensembles [1811.08209, Gérardin et al.]

Set 2: Small volume, Schrödinger functional [2010.09539, ALPHA],[1805.07401, Fritzsch]

differ by higher order cutoff effects. f_V is of $\mathrm{O}(g_0^6)$ and unknown.

- Finite-size corrections applied to the isovector correlator.
- Correction for $t^\star < \frac{(m_\pi L/4)^2}{m_\pi}$: Hansen-Patella method [1904.10010][2004.03935]
  - Expansion in the pion winding number.
  - Using monopole parametrization of the electromagnetic pion form factor.
- Large distances: MLL [1105.1892, Meyer] [hep-lat/0003023, Lellouch and Lüscher]:
  - Compute difference between finite and infinite-volume isovector correlator
  - Based on the time-like pion form factor.
  - Applied at large Euclidean distances $t > t^\star$.
- This is the only correction applied to the lattice data!

- Separate extrapolations of isovector, isocalar and charm contributions.
- General fit ansatz, not possible to resolve all parameters at once:

$$\begin{aligned} a_\mu^{\mathrm{win,f}}(X_a, X_\pi, X_K) = {} & a_\mu^{\mathrm{win,f}}(0, X_\pi^{\mathrm{exp}}, X_K^{\mathrm{exp}}) \\ & + \beta_2\, X_a^2 + \beta_3\, X_a^3 + \delta\, X_a^2 X_\pi + \epsilon\, X_a^2 \log X_a \\ & + \gamma_1\, (X_\pi - X_\pi^{\mathrm{exp}}) + \gamma_2\, (f(X_\pi) - f(X_\pi^{\mathrm{exp}})) \\ & + \gamma_0 \left(X_K - X_K^{\mathrm{phys}} \right) \end{aligned}$$

$$\text{where} \quad X_a \sim a\,, \qquad X_\pi \sim m_\pi^2\,, \qquad X_K \sim m_K^2 + \frac{1}{2} m_\pi^2$$

- Light quark mass effects: $f(X_\pi) \in \{0;\ \log(X_\pi);\ X_\pi^2;\ 1/X_\pi;\ X_\pi \log(X_\pi)\}$
- Final result and uncertainties from model average.

Chiral-continuum extrapolations: The intermediate-distance window

Compare high-precision lattice determinations - based on [2206.06582, Cè et al.]

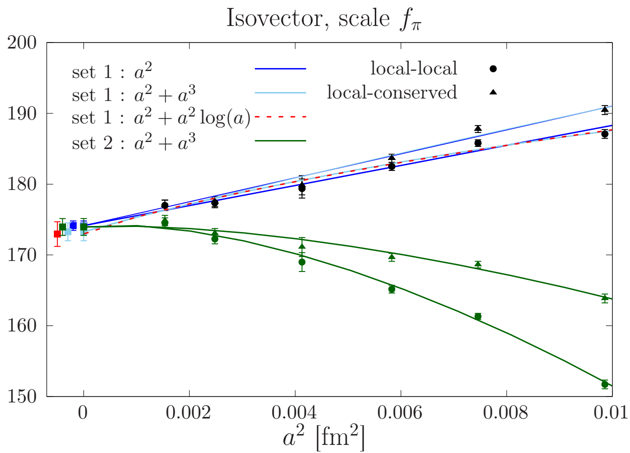

- Two sets of equally valid improvement coefficients.
- No cutoff effects of $\mathrm{O}(a^3)$ resolved for Set 1.
- Independent extrapolations compatible in the continuum $\rightarrow$ strong cross-check of our extrapolations.
- No sign of modification $a^2 \rightarrow (\alpha_{\mathrm{s}}(1/a^2))^{\hat{\Gamma}} a^2$ [1912.08498, Husung et al.]

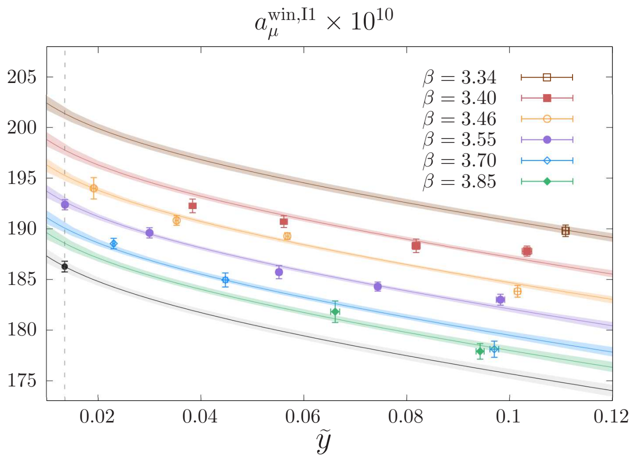

- f_π rescaling, local-local current and Set 1.
- Curvature in $\tilde{y} = \frac{m_\pi^2}{8\pi f_\pi^2}$ is needed to describe the data.
- Singular fit ansatz favored, also found in [2110.05493, Colangelo et al.]
- Variation in the chiral extrapolation does not change the result significantly.

$$a_\mu^{\mathrm{win}}(\tilde{y}) = \gamma_1\,(\tilde{y} - \tilde{y}^{\mathrm{exp}}) + \gamma_2\,(f(\tilde{y}) - f(\tilde{y}^{\mathrm{exp}}))\,, \qquad f(\tilde{y}) \in \{0;\ \log(\tilde{y});\ \tilde{y}^2;\ 1/\tilde{y};\ \tilde{y}\log(\tilde{y})\}$$

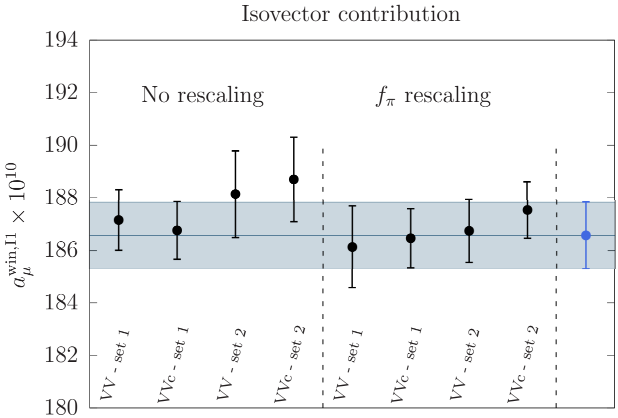

- Eight combinations of discretization and improvement procedures.
- Model averages in each category to determine systematic uncertainty from choice of fit model. [2008.01069, Jay and Neil]
- Final result by combining L and C of Set 1 with f_π-rescaling.

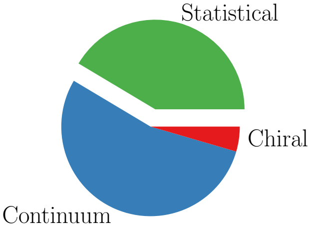

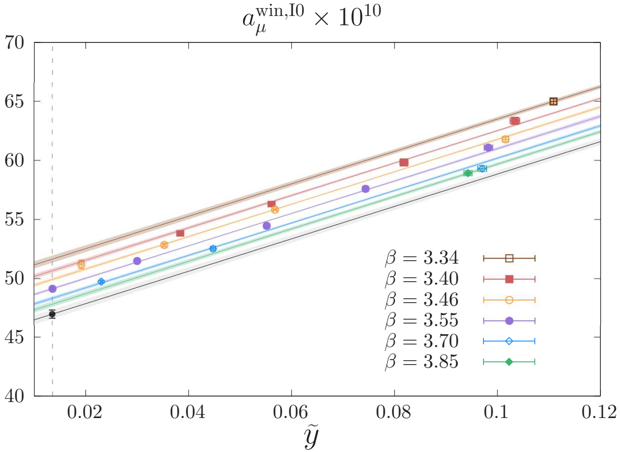

- Choose non-singular fit ansatz, $f(X_\pi) \in \{0;\ X_\pi^2;\ X_\pi \log(X_\pi)\}$
- Includes disconnected contribution: Driven to gauge noise [2203.08676, Cè et al.].
- Charm contribution not included at this stage.

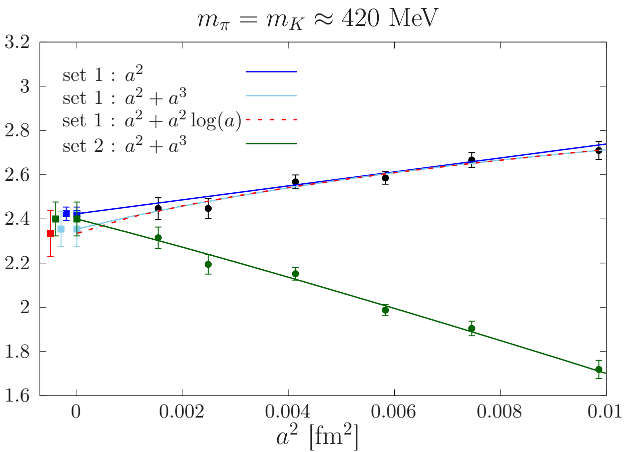

- Charm quark included in partially-quenched setup.
- Mass-dependent renormalization scheme.
- Effect of missing charm loops estimated to be $< 0.02\%$ for a_μ^{win} and at the per-mil level for a_μ^{hvp} [2206.06582, Cè et al.].
- Explicit, non-perturbative test is complicated with Wilson quarks (additive renormalization, am_c effects in the sea).

Isospin breaking corrections

- $\mathrm{QED_L}$-action [0804.2044, Hayakawa and Uno] for IR regularisation, Coulomb gauge

- Reweighting based on perturbative expansion [1303.4896, de Divitiis et al.] in $\Delta\varepsilon = \varepsilon - \varepsilon^{(0)} = (\Delta m_\mathrm{u}, \Delta m_\mathrm{d}, \Delta m_\mathrm{s}, \Delta\beta = 0, e^2)$:

$$C = C^{(0)} + \sum_{f=\mathrm{u,d,s}} \Delta m_f \, C^{(1)}_{\Delta m_f} + e^2 \, C^{(1)}_{e^2} + O(\varepsilon^2)$$

- Mesonic two-point functions $C = \langle \mathcal{M}_2 \mathcal{M}_1 \rangle$:
(quark-connected contribution, IB effects in valence quarks)

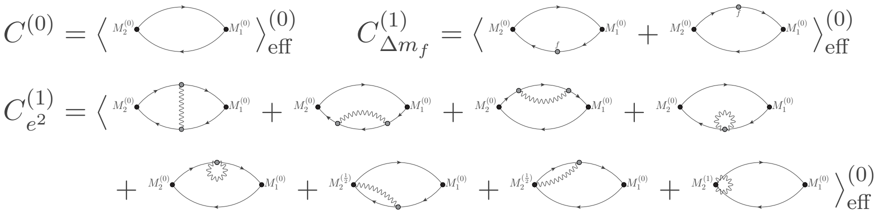

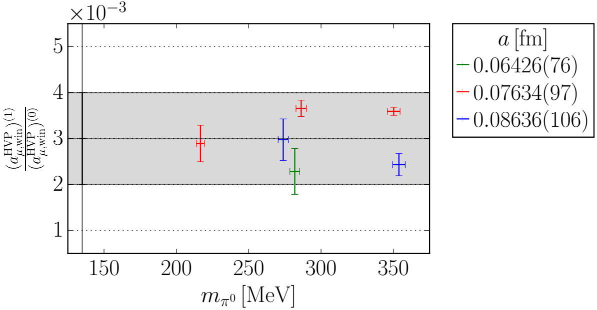

To be considered in the future:

- QED finite-volume effects.
- Quark-disconnected and sea-quark contributions.
- IB in scale setting [2212.07176, Segner et al.].

- Ongoing effort [2112.00878, Risch and Wittig]: Uncertainty on relative correction $0.3(1)\%$ doubled in final result for a_μ^{win}.
- Up-to-date overview in Andreas Risch's talk at the workshop *Converging on QCD+QED prescriptions* at Higgs Centre Edinburgh.
- Complementary approach [2209.02149, Biloshytskyi et al] employs coordinate space methods, similar to the HLbL contribution.

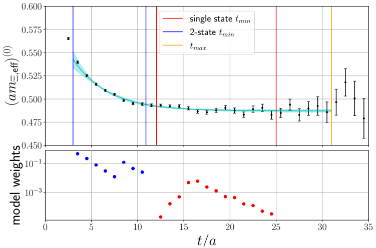

- Scale setting from the baryon spectrum. Currently most precise candidate: The Ξ (as in pure QCD in [2211.03744, Bali et al.]).

$\leftarrow$ Isosymmetric contribution at $m_\pi = 215\,\mathrm{MeV}$ and $a \approx 0.076\,\mathrm{MeV}$.

$\Downarrow$ First-order contributions $am^{(1)}_{\mathrm{eff},a\Delta m_s}$ and $am^{(1)}_{\mathrm{eff},e^2}$

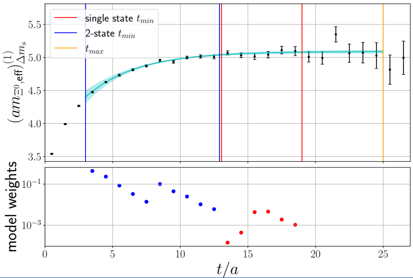

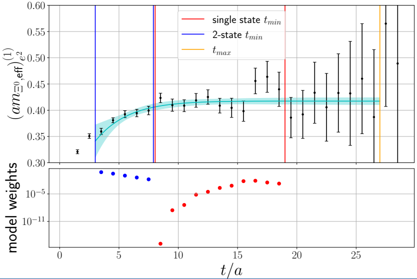

Blinding

- The community agreed on blinded analyses for a_μ^{hvp} to reduce biases.
- We have published results for a_μ^{hvp} and a_μ^{win} on a large number of ensembles: Could not prevent deliberate unblinding.
- We decided to introduce blinding at the stage of the analysis by modification of the QED kernel function $\widetilde{K}(t)$ in the integrand of the TMR:
  - Artificial cutoff effects (one kernel for each value of β).
  - Multiplicative offset.
  - ...? I don't know any details.
- Use five different sets modified of kernels.

Blinding strategy

- Unblinding strategy:
  1. Cross-check results between different analyses.
  2. Agree on final analysis. Freeze setup.
  3. Relative unblinding between the five sets of kernels in the continuum.
  4. Absolute unblinding of kernels / full analysis with true kernel.
- We tested this using mock data and another set of kernels.
- Our analysis is now blinded.

Noise reduction in the long-distance tail

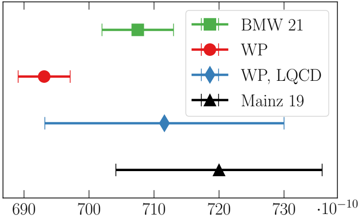

- 2.2% uncertainty: Dominated by statistical uncertainties of light quark contribution:

$$\frac{\Delta G^{\mathrm{I1}}(t)}{G^{\mathrm{I1}}(t)} \propto \exp\left[(m_{\mathrm{V}} - m_\pi)t\right]$$

- Variance reduction is needed to reach sub-percent precision.

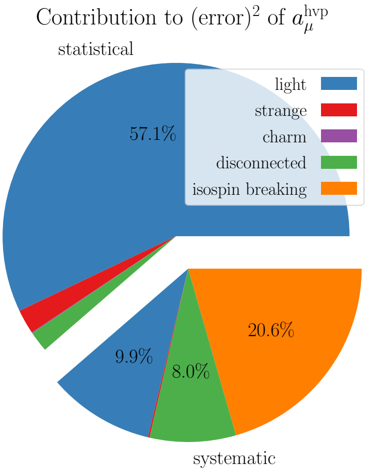

- Employ Low Mode Averaging (LMA) [hep-lat/0106016, Neff et al.][hep-lat/0402002, Giusti et al.][hep-lat/0401011, DeGrand et al.][...] to reduce the variance of the isovector contribution.

- Split up the quark propagator ($Q = \gamma_5 D_{\mathrm{W}}$)

$$Q^{-1} = Q^{-1}(\mathbf{P}_{\mathrm{L}} + \mathbf{P}_{\mathrm{H}}) = \sum_{i=1}^{N_{\mathrm{L}}} \frac{1}{\lambda_i} v_i v_i^{\dagger} + Q^{-1}\mathbf{P}_{\mathrm{H}}$$

  in low and high mode contributions using the projectors

$$\mathbf{P}_{\mathrm{L}} = \sum_{i=1}^{N_{\mathrm{L}}} v_i v_i^{\dagger}\,, \qquad \mathbf{P}_{\mathrm{H}} = \mathbf{1} - \mathbf{P}_{\mathrm{L}}$$

  with the eigenmodes v_i and the (real) eigenvalues λ_i of Q.

- Even-odd preconditioning reduces memory by factor 2 [1004.2661, Blossier et al.].

- The connected two-point function contains two quark propagators

$$C_{AB}(x_0, y_0) = \sum_{\mathbf{x},\mathbf{y}} \left\langle \mathrm{Tr}\left[\gamma_5 \Gamma_A Q^{-1}(x,y) \gamma_5 \Gamma_B Q^{-1}(y,x)\right] \right\rangle$$

  with γ_5 insertions because we use Q.

- We get four terms contributing to C_{AB}, with $t \equiv x_0 - y_0$,

$$C(t) = C^{ll}(t) + C^{hl}(t) + C^{lh}(t) + C^{hh}(t) \, ,$$

  each can be defined and computed separately:

  - Evaluate $C^{ll}(t)$ with **full volume average**.
  - Evaluate $C^{hl}(t) + C^{lh}(t)$ by inversion on eigenmodes (alternative: stochastic).
  - Evaluate C^{hh} stochastically.

- Use Truncated Solver Method [0910.3970, Bali et al.] to reduce cost of inversions.

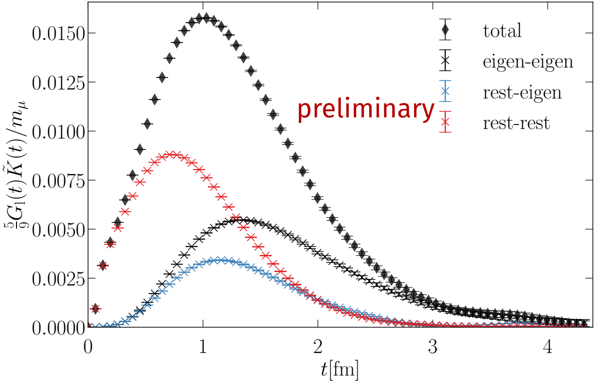

- Light-connected contribution to a_μ^{hvp} for $m_\pi \approx 129\,\mathrm{MeV}$ in a $12.4\,\mathrm{fm} \times (6.2\,\mathrm{fm})^3$ box at $a = 0.064\,\mathrm{fm}$.
- 800 eigenmodes of the even-odd preconditioned Dirac-Wilson operator $\gamma_5 \hat{D}$.
- All-to-all evaluation of low eigenmodes dominates correlator and its variance for $t > 1.5\,\mathrm{fm}$.

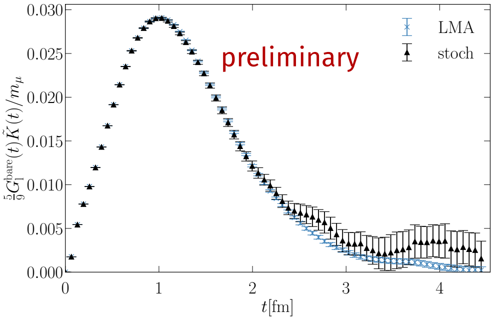

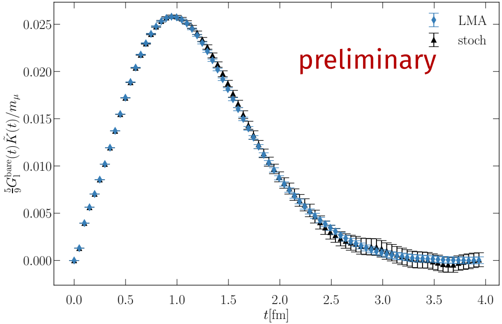

- Illustration of increase in precision on ensembles close to the physical point.
- **Left**: $m_\pi \approx 129\,\mathrm{MeV}$, $a = 0.064\,\mathrm{fm}$. **Right**: $m_\pi \approx 174\,\mathrm{MeV}$, $a = 0.050\,\mathrm{fm}$.
- Currently limited by autocorrelation on finer ensemble.

VARIANCE REDUCTION: SPECTROSCOPY

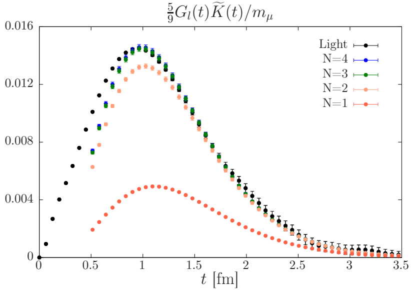

- Spectral decomposition of the vector correlator:

$$G_l(t) = \sum_n |A_n|^2 \mathrm{e}^{-E_n t}\,, \qquad E_n = 2\sqrt{m_\pi^2 + k^2}$$

- Dedicated spectroscopy computation to determine A_n and E_n at $200\,\mathrm{MeV}$ [1808.05007, Andersen et al.] [1904.03120, Gérardin et al.]. Impose bound on long-distance tail.

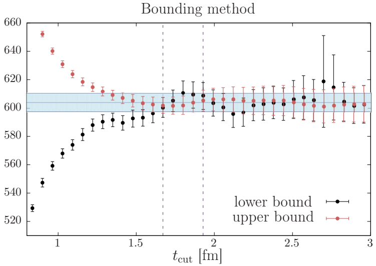

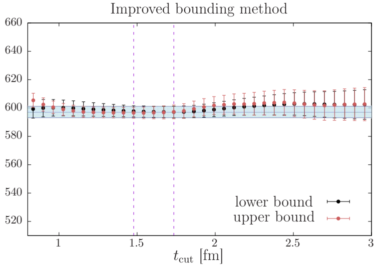

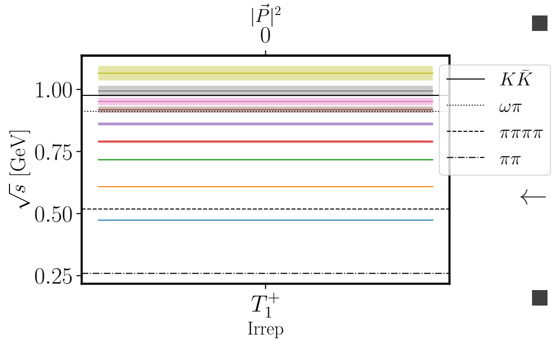

- Extend the spectroscopy computation to close-to-physical masses: E250 with $m_\pi \approx 129\,\mathrm{MeV}$ at $a = 0.064\,\mathrm{fm}$ [2112.07385, Paul et al.].

$\leftarrow$ Two-pion, zero-momentum energy levels on E250.

- Expect more states to contribute significantly compared to $m_\pi = 200\,\mathrm{MeV}$.

- Reconstruction in progress, not yet combined with $G(t)$.
- Same data will be used for the computation of the pion transition form factor to correct for finite-size effects with less model dependence.

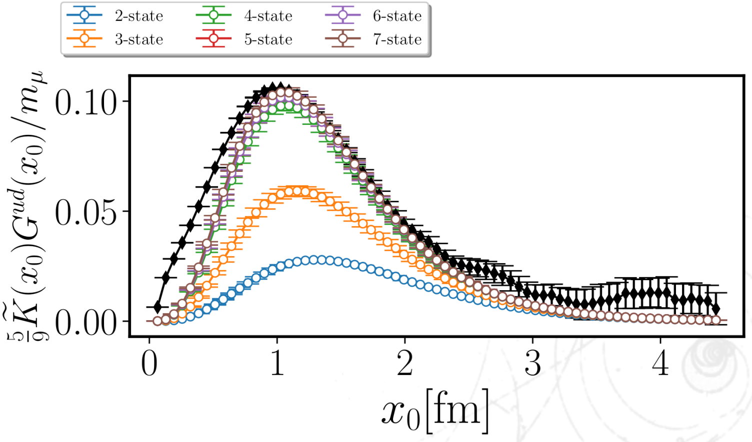

- Reconstruction of the light-connected TMR correlator at long distances at close-to-physical pion mass [PoS LATTICE2022 073, Paul et al].

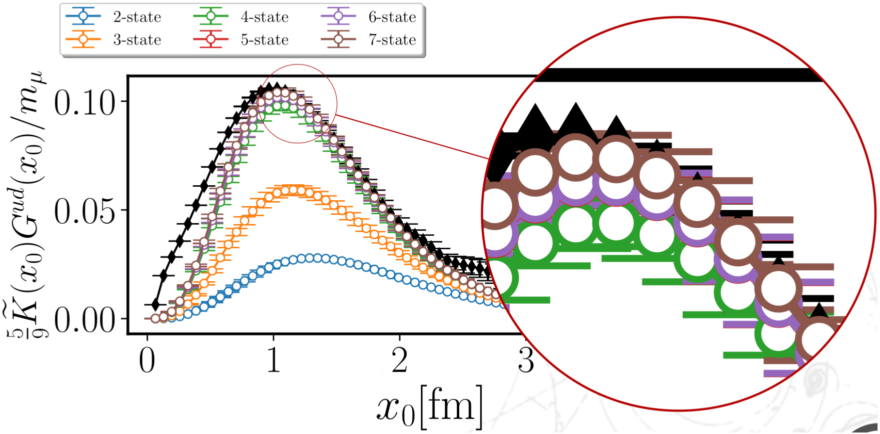

- Reconstruction of the light-connected TMR correlator at long distances at close-to-physical pion mass [PoS LATTICE2022 073, Paul et al].

Variance reduction: comparison

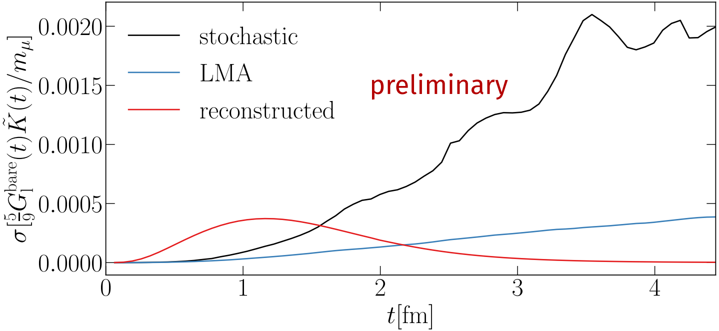

- Comparison of statistical uncertainties of the TMR correlator based on stochastic evaluation, reconstruction and LMA at m_π^{phys}.
- Significantly less noise in LMA correlator.
- Noise in reconstructed correlator grows only **linearly**.

Strange quark mass mistuning

- We keep $2am_\mathrm{l} + am_\mathrm{s} = \mathrm{const}$ on our ensembles.
- This implies (with $f_{K\pi} = \frac{2}{3}(f_K + \frac{1}{2}f_\pi)$)

$$X_K \in \{\Phi_4,\, y_{K\pi}\} \sim \mathrm{const} \quad \text{where} \quad \Phi_4 = 8t_0(m_K^2 + \frac{1}{2}m_\pi^2)\,, \qquad y_{K\pi} = \frac{m_K^2 + \frac{1}{2}m_\pi^2}{8\pi f_{K\pi}^2}$$

  up to $\mathrm{O}(a)$ and NLO χPT effects.
- We correct for the small deviation $\Delta X_K = X_K^{\mathrm{phys}} - X_K$ in the global fit.
- No independent variation of the Kaon mass: fit parameter γ_0 not stable.

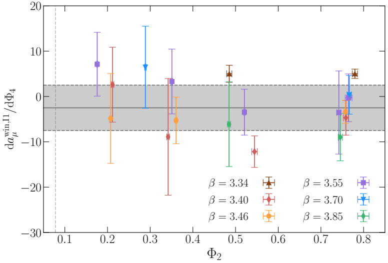

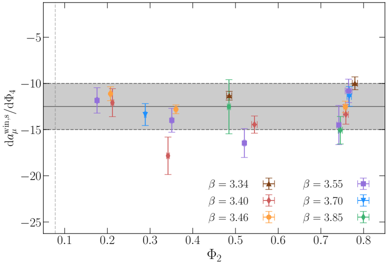

- Explicit computation of $\frac{\mathrm{d}\langle a_\mu^{\mathrm{win}}\rangle}{\mathrm{d}X_K}$.
- Based on mass-derivatives $\frac{\mathrm{d}\langle \mathcal{O}\rangle}{\mathrm{d}m_{\mathrm{q},i}}$ and a first-order Taylor expansion [1608.08900, Bruno et al.].
- Results confirmed by pheno estimates.
- Use results as priors for fit parameter γ_0.
  - No significant strange quark mass dependence for $a_\mu^{\mathrm{win,I1}}$.
  - Negative contribution for $a_\mu^{\mathrm{win,s}}$.
- Large uncertainties for $\frac{\mathrm{d}\langle a_\mu^{\mathrm{hvp,I1}}\rangle}{\mathrm{d}X_K}$.

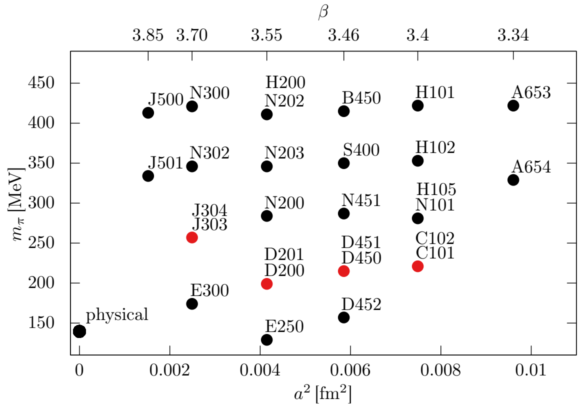

- Include ensembles with near-physical strange quark mass [RQCD, 1606.09039] and $m_\pi = \mathrm{O}(200\,\mathrm{MeV})$ in global fit.
- Slight variation of $\Phi_4 = 8t_0(m_K^2 + \frac{1}{2}m_\pi^2)$ due to change in m_s at these points in parameter space.
- Very mild dependence of light-connected correlation function on sea strange mistuning.

Strange quark mass dependence of a_μ^{hvp}

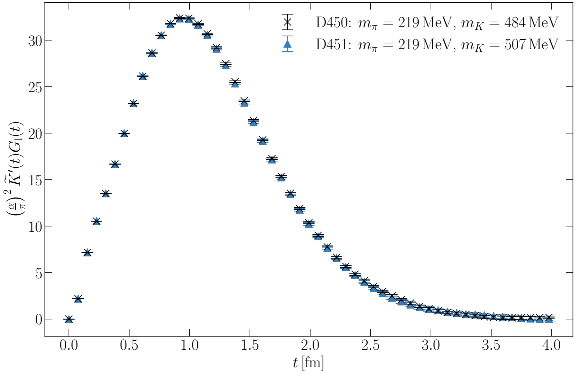

- Include ensembles with near-physical strange quark mass [RQCD, 1606.09039] and $m_\pi = \mathrm{O}(200\,\mathrm{MeV})$ in global fit.
- Slight variation of $\Phi_4 = 8t_0(m_K^2 + \frac{1}{2}m_\pi^2)$ due to change in m_s at these points in parameter space.
- Very mild dependence of light-connected correlation function on sea strange mistuning.

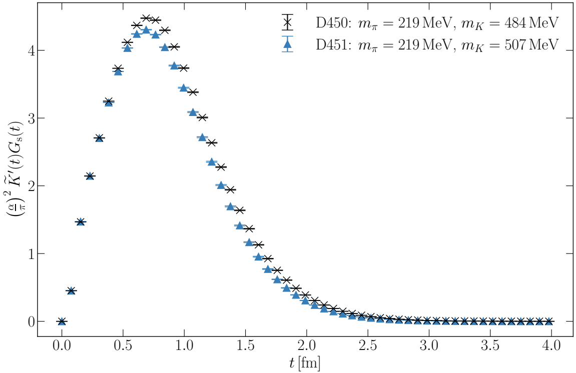

- Include ensembles with near-physical strange quark mass [RQCD, 1606.09039] and $m_\pi = \mathrm{O}(200\,\mathrm{MeV})$ in global fit.
- Slight variation of $\Phi_4 = 8t_0(m_K^2 + \frac{1}{2}m_\pi^2)$ due to change in m_s at these points in parameter space.
- Very mild dependence of light-connected correlation function on sea strange mistuning.

Scale setting

- Scale enters via muon mass in $\tilde{K}(t)$. Determine the scale dependence via

$$\frac{\partial (a_\mu^{\mathrm{hvp}})^i}{\partial_\Lambda} = \left(\frac{\alpha}{\pi}\right)^2 \sum_0^\infty dt \left[\left(\frac{\partial}{\partial_\Lambda} \widetilde{K}(t) \right) W^i(t;t_0;t_1) + \widetilde{K}(t) \left(\frac{\partial}{\partial_\Lambda} W^i(t;t_0;t_1) \right) \right] G(t)$$

- Using a parametrization of the R-ratio, the Mainz group estimated $\frac{\Delta a_\mu^{\mathrm{hvp},\Lambda}}{a_\mu^{\mathrm{hvp}}} \approx 1.8 \frac{\Delta\Lambda}{\Lambda}$ [1705.01775, Della Morte et al.] $\rightarrow$ What about the windows?

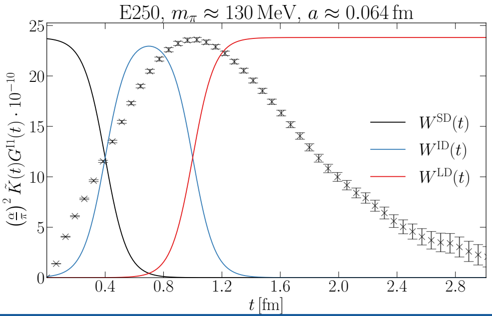

- Scale enters via muon mass in $\tilde{K}(t)$. Determine the scale dependence via

$$\frac{\partial (a_\mu^{\mathrm{hvp}})^i}{\partial_\Lambda} = \left(\frac{\alpha}{\pi}\right)^2 \sum_0^\infty dt \left[\left(\frac{\partial}{\partial_\Lambda}\widetilde{K}(t)\right) W^i(t;t_0;t_1) + \widetilde{K}(t)\left(\frac{\partial}{\partial_\Lambda} W^i(t;t_0;t_1)\right)\right] G(t)$$

- Using a parametrization of the R-ratio, the Mainz group estimated $\frac{\Delta a_\mu^{\mathrm{hvp},\Lambda}}{a_\mu^{\mathrm{hvp}}} \approx 1.8 \frac{\Delta\Lambda}{\Lambda}$ [1705.01775, Della Morte et al.] $\rightarrow$ What about the windows?

- My **rough estimates** for $\frac{\Delta (a_\mu^{\mathrm{hvp},\Lambda})^i \Lambda}{(a_\mu^{\mathrm{hvp}})^i \Delta\Lambda}$ at m_π^{phys}:

$\delta a_\mu^{\mathrm{hvp}}$	$\delta (a_\mu^{\mathrm{hvp}})^{\mathrm{SD}}$	$\delta (a_\mu^{\mathrm{hvp}})^{\mathrm{ID}}$	$\delta (a_\mu^{\mathrm{hvp}})^{\mathrm{LD}}$
1.8	0.0	0.5	2.7

- Need a highly precise scale setting for precision in a_μ^{hvp}.

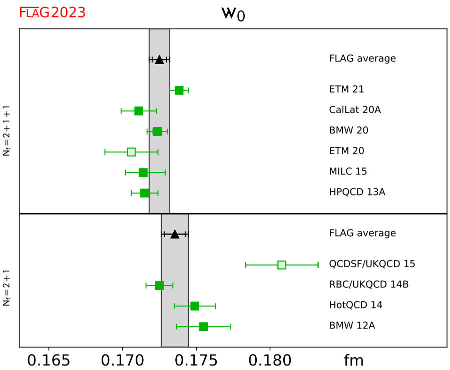

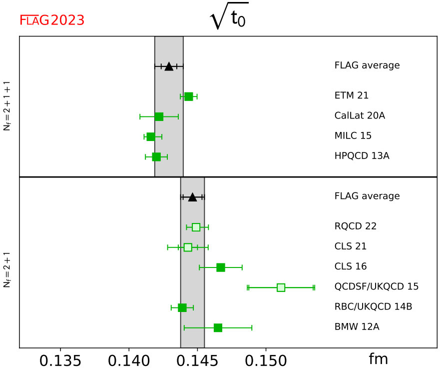

- Flow scales are not in good agreement within each set of $2+1$ and $2+1+1$.
- Differences between $2+1$ and $2+1+1$ larger than expected.
- This can have a significant influence on a_μ^{hvp}.

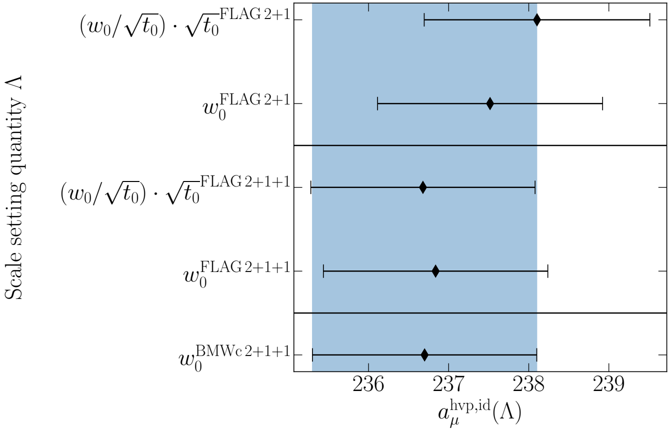

- Shift the result of [2002.12347, BMWc] based on estimated scale dependence.
- $(\sqrt{t_0}/w_0)^{\mathrm{FLAG\,2+1+1}}$ from [EMTc, 2104.06747][HPQCD, 1303.1670].
- Ignored possibly larger errors on Λ.

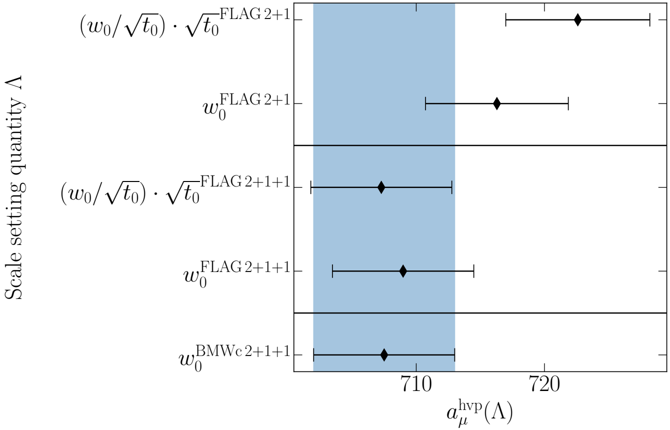

- Shift the result of [2002.12347, BMWc] based on estimated scale dependence.
- $(\sqrt{t_0}/w_0)^{\mathrm{FLAG\,2+1+1}}$ from [EMTc, 2104.06747][HPQCD, 1303.1670].
- Ignored possibly larger errors on Λ.
- The choice of Λ has a significant impact!

Work that I did not talk about

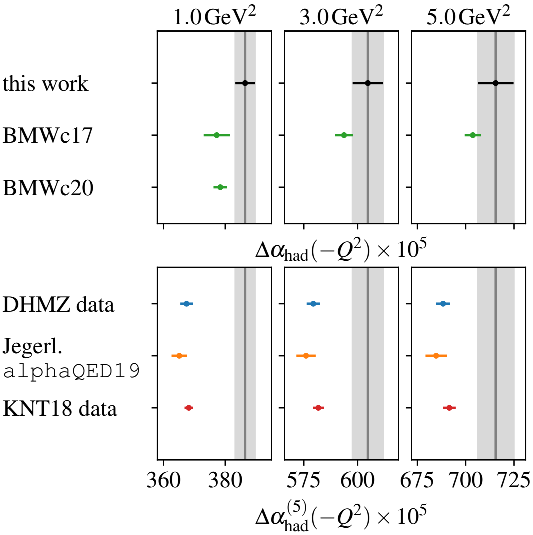

- Running of $\Delta\alpha_{\mathrm{had}}$ computed in [2203.08676, Cè et al.].
- Significant tension with data-driven estimates at low Q^2.
- A future update would profit from all improvements for a_μ^{hvp}.

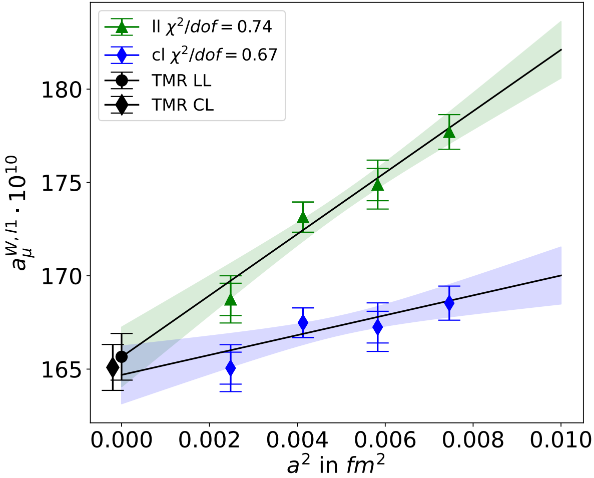

- The covariant-coordinate space (CCS) method [1706.01139, Meyer] offers an alternative to the TMR to compute a_μ^{hvp} and a_μ^{win}.
- Computation of a_μ^{win} at $350\,\mathrm{MeV}$ pion mass in [2211.15581, Chao, Meyer, Parrino].
- Good agreement with TMR.

Outlook

- We are performing a blinded analysis.
- Reduction of statistical uncertainties underway.
- Spectroscopy and variance reduction techniques help to significantly improve our precision at physical pion mass.
- We started investigating sub-leading systematic effects, such as strange quark mistuning.
- Scale setting limits our attainable precision.
- Investigation of isospin breaking effects ongoing.

Backup

Comparison with lattice results for $a_\mu^{\text{win,iso}}$

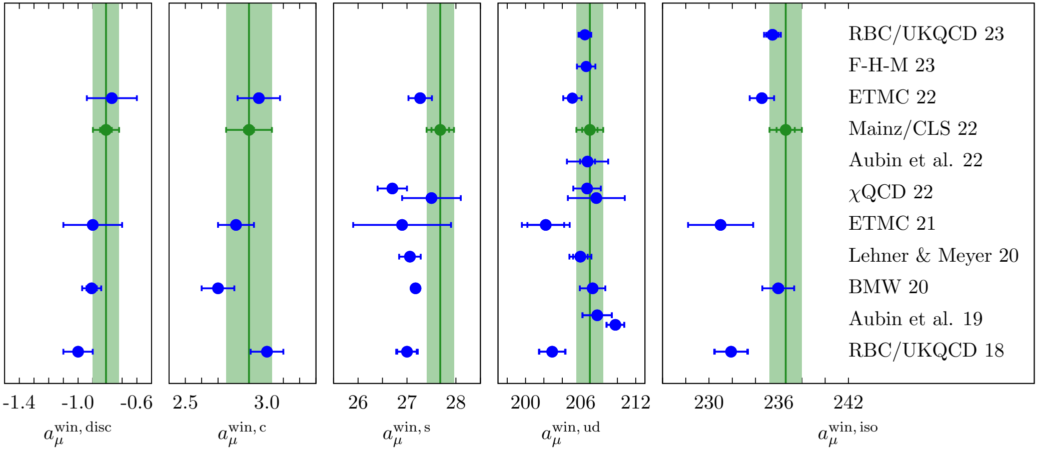

$$a_\mu^{\text{win,iso}} = a_\mu^{\text{win,I1}} + a_\mu^{\text{win,I0}} + a_\mu^{\text{win,c}} = (236.60 \pm 0.79_{\text{stat}} \pm 1.13_{\text{syst}} \pm 0.05_{\text{Q}}) \times 10^{-10}$$